Electronic Supplementary Material (ESI) for Nanoscale.

Supplementary Information

E-mail:

*To whom correspondence should be addressed

Technical details of the *ab initio* calculations

Our first-principles calculations are performed at the Kohn-Sham[1] DFT[2] level. We employ the SIESTA code[3] with different implementations of the exchange-correlation functional: i) the well-known spin-polarized local density approximation (LDA functional), as parameterized by Perdew-Zunger[4] and based on Ceperley-Alder simulations of the electron gas;[5] ii) the spin-polarized generalized gradient approximation (GGA), as implemented by Perdew, Burke and Ernzerhof (PBE functional);[6] iii) the fully nonlocal van der Waals functional (vdW-DFT) proposed by Dion *et al.*,[7] as implemented self-consistently by Román-Pérez and Soler[8] in SIESTA. Several parametrizations exist for this functional. In this work, we employ that proposed by Klimes, Bowler, and Michaelides (KBM functional).[9] The first functional (LDA) is used only for testing and benchmarking the performance of several DFT implementations; the main results of our paper have been obtained with the PBE and KBM functionals.

The SIESTA code employs norm-conserving pseudopotentials to describe the core electrons,[10] in their fully separable form.[11] Our pseudopotentials include non-linear partial core corrections[12] which are known to be important for zinc, and were generated self-consistently for each of the XC-functionals employed. The $3d-$manifold is explicitly included in the active valence space. Tests were performed to ensure that eigenvalues and excitations energies for several atomic configurations reproduced the all-electron results to better than 1 mRy.

SIESTA uses a flexible linear combination of numerical atomic orbitals as basis set, allowing unlimited multiple-zeta and angular momenta, as well as polarization and off-site orbitals. In order to limit the range of the basis pseudo-atomic orbitals, they are slightly excited by a common energy shift and truncated at the resulting radial node. In our calculations, the size of the basis set was double-zeta plus two polarization orbitals (DZP2), resulting in a total of eight basis functions per atom.

The basis functions and the electron density are projected into a uniform real-space grid in order to calculate the Hartree and exchange-correlation potentials and matrix elements.

Table S1: Equilibrium bond distance d and cohesive energy E_{coh} of the Zn_2 dimer, and lattice constants a, c and cohesive energy E_{coh} of bulk Zn, as predicted by several exchange-correlation functionals, are compared to either experimental results or other theoretical calculations. Because experimental values about the spectroscopic constants of the dimer do not agree with each other, we choose to show high-level coupled-cluster benchmark results for comparison purposes, taken from Reference.[13] Experimental results for bulk Zn are taken from[14]

Zn_2	d (Å)	E_{coh} (eV)
LDA	2.880	0.097
PBE	3.248	0.027
KBM	3.990	0.010
CCSD(T)	3.9-4.0	0.011-0.013
Zn(bulk)	a,c (Å)	E_{coh} (eV)
LDA	2.601, 4.828	1.78
PBE	2.697, 5.026	1.12
KBM	2.713, 5.148	0.98
Exp.	2.6648, 4.9467	1.30

The grid fineness is controlled by the energy cutoff of the plane waves that can be represented in it without aliasing, so this quantity is the analogue of the energy cutoff of typical plane-wave codes. In our work we have found that a cutoff of 200 Ryd suffices to converge energies, dipole moments and other electronic properties with respect to the grid resolution.

All equilibrium cluster geometries were obtained from unconstrained conjugate-gradients structural relaxation using DFT forces. The structures were relaxed until the force on each atom was smaller than 0.01 eV/Å.

The accuracy of our computational settings for both the dimer and bulk limits is shown in Table S1. Because of the closed-shell electronic configuration of Zn, the dimer is bound only by weak van der Waals' forces, which poses serious difficulties for theoretical calculations. Many of them resulted in a negative dissociation energy in the past, and experimental results also show scattered data. Only the most accurate levels of theory have led to consistent and reproducible results with little scattering, and these are shown in the Table as a benchmark reference. Not surprisingly, only the KBM functional can describe the dimer with a good accuracy, comparable indeed to the accuracy of more elaborate CCSD(T) methods (coupled

cluster calculations with single and double excitations included, and a perturbative estimation of triple excitations). The LDA results in a very substantial overbinding, which is only partially alleviated in PBE calculations. In the bulk limit, on the contrary, both PBE and KBM result in accurate reproduction of experimental values, with PBE performing slightly better. Because of its higher accuracy for bulk properties and its lower computational expense, we have performed the main calculations of this paper with the PBE functional, although performing an extensive comparison of PBE and KBM results for clusters with up to $N = 21$ atoms and some other selected sizes. The results, shown in the main paper, demonstrate the similar performance of PBE and KBM for most sizes and a nice reproduction of the relative abundances observed in the experimental mass spectra. Independent benchmark bulk calculations performed by Janthon *et al.*[15] with the VASP code confirm the high accuracy of the PBE functional for the particular case of zinc. Also, a previous work[16] already demonstrated that vdW-like bonding in small Zn clusters persists only up to $N = 4$.

For a few selected clusters, chosen from those exhibiting unusual structural or electronic behaviors as discussed in the main text, we additionally performed a comparison with results obtained using the VASP code[17,18] with the PBE functional. VASP employs a plane-waves basis set instead of numerical pseudoatomic orbitals, and the core interactions are treated by means of the projector-augmented wave (PAW) approach instead of pseudopotentials. In all cases the agreement with our SIESTA setup was essentially perfect, reinforcing the confidence in the results obtained with SIESTA. In the end, the accuracy of the SIESTA results for clusters is demonstrated by the nice reproduction of photoemission results (seen in the main paper) and also of mass abundance spectra.

We have additionally double-checked our results against TURBOMOLE[19] and G09[20] codes, both of which have high accuracy standards in the quantum chemistry community. We have chosen Zn_{10}^{-} as a test system to perform the benchmark comparisons. Specifically, we have considered five different structural isomers to check their energetic ordering (see fig. 1). In first place, we have performed single-point all-electron PBE-TURBOMOLE

calculations at the SIESTA optimal geometries of Zn_{10}^- anion in order to check the different basis sets provided in TURBOMOLE, from "def-SV(P)" to "def2-QZVPPD", and also with two different grids (called "m3" and "m5" in TURBOMOLE) to check the quality of the performed Fourier transforms. The results show that the "m3" grid with the def2-TZVPD basis set already provide well converged results for the binding energy, HOMO-LUMO gap, and vertical detachment energy. With this assertion we specifically mean that going from def2-TZVPD/m3 to def2-QZVPPD/m5 calculations the HOMO-LUMO gap and vertical detachment energies change by only 0.01 eV, and the binding energy per atom changes by less than 0.01 eV/atom. So the TURBOMOLE geometry optimizations have been performed at the def2-TZVPD/m3 level. We have done similar single-point PBE energy calculations with the G09 code employing Pople basis sets, to conclude that 6-31+g(d) basis offers well converged results: augmenting the basis to 6-311+g(2d) produces again changes of less than 0.01 eV/atom in binding energies, and of less than 0.01 eV in HOMO-LUMO gap and VDE values. The G09 optimizations have then been performed with the 6-31+g(d) basis. The choice of Pople basis sets allows to test a different basis set, not employed in the TURBOMOLE calculations.

Taking the optimal SIESTA structures as an input for TURBOMOLE, we have then optimized the geometries of the five isomers of Zn_{10}^- with TURBOMOLE, also at the all-electron level. Each separate optimization took only about 10 steps and finished in about one hour, which is already an indication that SIESTA and TURBOMOLE optimal structures are very close. A detailed analysis (performed on the GM structure for instance, but the results are similar for the five isomers) shows that the only significant difference is a contraction by 0.036 Å in the average bond distance, i.e. TURBOMOLE optimal geometries are slightly more compact.

We have also performed single-point SIESTA calculations on the TURBOMOLE optimal geometries. It is interesting to notice that both codes produce exactly the same vertical detachment energy when calculated at the same geometry. At the SIESTA optimal geometry

both codes produce a value of 1.87 eV for the GM structure, while at the TURBOMOLE optimal geometry both codes produce 1.81 eV. So both codes seem to predict the same electronic properties if the external nuclear potential is the same, so the only important difference is indeed the contraction in average bond distance, which is a 1.3% difference in percentage value.

Concerning G09 optimizations, we found that optimal G09 and TURBOMOLE geometries are very similar, although G09 is slightly closer to SIESTA results (G09 structures are 1.1% more compact on average than SIESTA geometries, instead of the 1.3% difference obtained with TURBOMOLE). Being the difference in bond distances smaller, the G09 result for the vertical detachment energy (1.84 eV) also agrees better with the SIESTA result of 1.87 eV. Finally, we performed additional single-point G09 calculations with the 6-311+g(2d) basis, on the 6-31+g(d) optimized structures, which in quantum chemical standard notation is a pbepbe/6-311+g(2d)//pbepbe/6-31+g(d) calculation. This last calculation is done to check the energetic ordering of isomers with a more complete basis. As shown in Figure 1, all the different codes predict the same energetic ordering and similar energy differences, irrespective of basis set and of the pseudopotential approximation employed in SIESTA. Some fluctuations between codes are always to be expected, but it seems that the vertical detachment energy typical fluctuation is of the order of only 0.05 eV or less, and the bond distance fluctuation is of about 1%. Energy differences are also consistent between codes, and although SIESTA results are systematically lower (probably related to the longer average bond distance), the differences remain of the order of 0.01 eV/atom or less.

These detailed comparisons demonstrate that SIESTA-PBE is very close to both TURBOMOLE-PBE or G09-PBE. SIESTA calculations produce an VDE value of 1.87 eV, which is in slightly better agreement with the experimental value of 1.91 eV, so SIESTA is slightly more accurate than TURBOMOLE or G09 in this sense. Nevertheless, we emphasize that the only meaningful conclusion in our opinion is that all codes are pretty close. Small fluctuations in the results of several codes are expected and observed in most comparisons, and it is

much more difficult to discuss them. We can state that it needed vary careful optimization of the SIESTA basis and pseudo to get it to work that well, and that we do not have the possibility to tweak TURBOMOLE or G09 basis sets in a similar way. We can not be sure if the better agreement between SIESTA and experiment is just a fortunate issue with the employed pseudopotential, or a result of our careful basis optimization, but what we can assert is that SIESTA-PBE compares slightly better with experiment, so it is certainly well suited to deal with our particular problem.

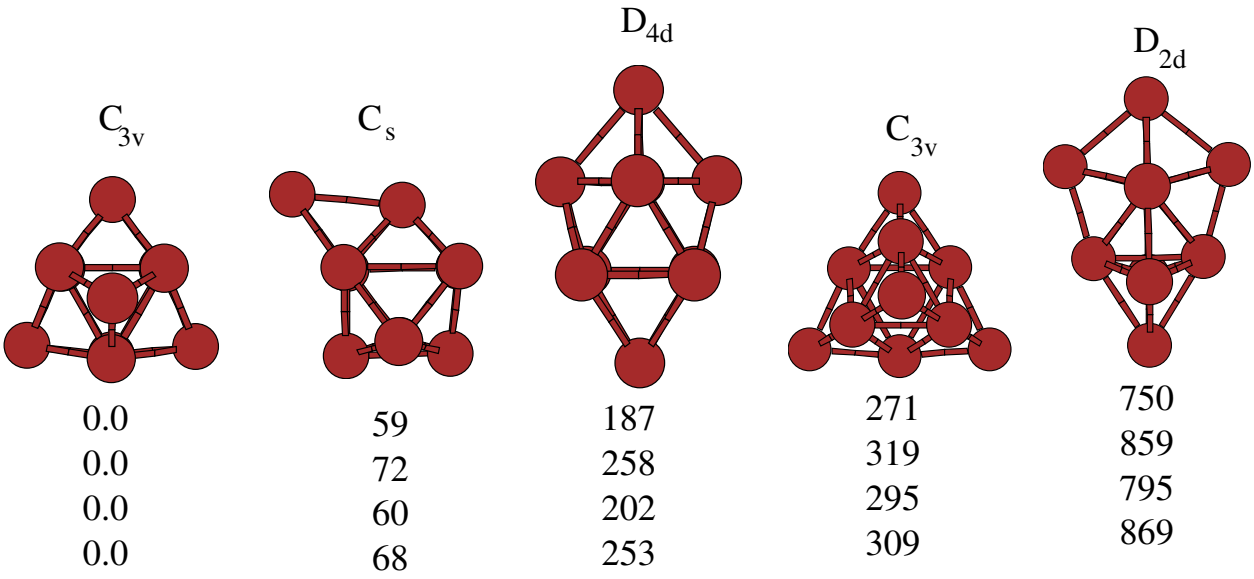

Figure S1: Structures and point group symmetries of five selected isomers of Zn_{10}^{-}. The numbers below each isomer give the energy difference with respect to the GM structure: 1st row (SIESTA results); 2nd row (TURBOMOLE results with def2-TZVPD basis); 3rd row (G09 results with 6-31+g(d) basis); 4th row (pbepbe/6-311+g(2d)//pbepbe/6-31+g(d) G09 results).

Additional technical details about the optimization runs

For each cluster size and for a given Gupta potential, we always performed three independent BH runs, with different values of the temperature variable used in the acceptance Metropolis algorithm, and a fourth additional BH run in which the temperature is decreased from a high to a low value (a sort of "annealing BH" run). The four runs add up to a total of two

million BH steps.

Each of those four runs is started from a randomly generated structure, but this does not mean that there are only four starting points. The GMIN code includes a "restart" option that we have employed. When the energy does not improve after a user-specified number of steps (we used values between 20000 and 50000 steps) the run is re-seeded with a new random structure. So we can not specifiy a precise number of starting points, as it is decided by the code and is different for each size, but about 10 restarts are usual in each run. On average, that would result in 40 starting points.

The BH runs are performed for each different size, but the attribute "charge" is not present yet at the level of the employed Gupta potential. So the same structural databank is employed for cations, anions and neutrals of a given size. The three DFT optimization are "independent" in the sense that they are all started directly from the Gupta minima (instead of optimizing first the neutrals, and then using those DFT-optimized structures as an input for cations and anions).

The "size-comparison" for $N+1$ and $N-1$ clusters was performed as a final optimization stage directly at the DFT level. As no BH run is completely exhaustive, and also because 100 selected structures for DFT re-optimization may be not enough, this final step may help sometimes. We typically remove low-coordinated atoms, and add atoms at high-coordination sites, i.e. we perform this "size-comparison" check manually, which sometimes amounts to a lot of work. Moreover, we don't do it only with the current GM structure of the $N-$cluster, but also with the first few excited isomers. In the end, there may be up to 30 new structures generated this way. We also performed "charge-comparison" at the *ab initio* level any time that we observed that, starting from the same Gupta structure, anion and neutral (for instance) relax to different structures in the DFT optimization.

When these last steps find a new putative GM, it is always one that differs little from an already existing one (typically moving one adatom to one place to another, for example). In those cases, we have always checked that the new structure is a local minimum at the Gupta

level, i.e. the size-comparison step essentially complements the isomer-selection step, rather than providing new minima that are not on the Gupta data bank. This point is important to emphasize that the whole search is based on the structures located at the Gupta level, with little modifications. An example of GM structures located in this last size-comparison step is Zn_{55} and Zn_{55}^{-}, which both have adatoms on top of Zn_{54}.

To complete this part, we mention that the seeded BH runs (with a fixed core) mentioned in the main text were essential to locate the D_{2d} structures at sizes N =54 and 56. Both contain a 10-atom tetrahedron as core, and for some reason they were not located even after 2 million unconstrained BH steps. It was precisely the availability of experimental data and the bad initial agreement with photoemission spectra for those sizes that forced us to run some seeded-core constrained optimizations. We have found in our previous research more examples that show that tetrahedral spiky shapes are quite difficult to locate.

Additional details about the optimization of the potential

We provide here more details about the performance ranking of the potentials which might be useful to other researchers trying the approach. An interesting question is whether one should expect to find a single "best" Gupta potential for a given metal or rather just an optimal local region in parameter space. Our experience with Zn clusters leads us to conclude that, while there is a "best average potential", it is always advisable to employ also potentials in a local environment around the optimal parameters to enhance diversity. This is in fact expected because the Gupta potential is very simple and does not contain explicit representations of many effects which are very important in the physics of metal clusters, as for example electronic shell effects. All those complexities in the interactions are embedded into just two parameters in the reduced Gupta potential, so some fluctuations in the values of optimal parameters as a function of cluster size should be expected, and in our opinion

may be unavoidable unless a much more complex potential is employed. A related problem is whether one will be able to discern any smooth evolution of optimal parameters as a function of cluster size, or if such an evolution will be "blurred" by the fluctuations of optimal parameters as a function of size.

Concerning these interesting questions, we stress that we have used the averaged *ab initio* binding energy per atom of the six chosen cluster sizes to rank the potentials, so a first thing to point out is that we have not yet analyzed if different potentials are better in different size ranges. We preferred to have a better statistics by averaging the results of the six sizes. Nevertheless, the results confirm *a posteriori* that the size range considered in this paper is not wide enough yet to discern any sort of evolution in the optimal parameters. Our optimal potential should be considered "optimal on average", and there may be significant fluctuations (for example, due to electronic shell effects not present in a Gupta potential description) from the mean, which make impossible to discern a clear evolution in the optimal parameters as a function of size, and which suggest to use in practice not a single potential but several in a local average about the optimal one. This is precisely what we have done.

In the initial coarse grain procedure for optimizing the potential, in which the whole parameter space is sampled, there is a well defined region that clearly wins in the ranking, as mentioned in the main paper: the corner with high values of λ and small values of χ. The local minima produced by different potentials are very different in general, so the energy differences after DFT-reoptimization are significant. This initial procedure focuses the user clearly and neatly (without any confusion) towards that region of parameter space (as a side comment, the bulk parametrization is also within that region). Of course, when using a finer grain within that local region in a second step, different potentials are no longer so different as before and get closer in the ranking. Here the user should experiment himself, we have considered only the Zn system with this technique and we will have to experiment ourselves for other systems. There is not a clear recipe on how fine should the grid be made, but in order to be useful it should not be so fine that neighboring potentials in the grid are nearly

equivalent. The "best on average" potential corresponds to a maximum averaged binding energy per atom calculated after SIESTA optimization. If several potentials in a local region of parameter space around the "best" rank similarly, our advice would be to use several of those potentials as generators of reasonable structures.

As an useful addition to the interested reader, we include here the following information: we have observed that the λ parameter is much better fixed than χ by our procedure. Although this may be different for other systems, it seems to imply that the number of core atoms (the property controlled by λ) is a much stronger property, i.e. one affecting the energy to a more significant degree. The value $\lambda = 0.48$ is thus strongly fixed, as already values of 0.47 and 0.49 produce for many sizes structures with the wrong number of core atoms, and this is indeed one important reason why the bulk-fitted potential (with $\lambda = 46$) is so bad for clusters. χ, on the contrary, produces a smaller effect on the objective function (the energy), and although $\chi = 2$ is its optimal value according to our definition, values of up to $\chi = 50$ produce also good results. These results demonstrate something important: Zn clusters have a well defined value of the optimal number of core atoms, and changing that costs much energy; however, the amount of energy penalty induced by bond strain is not so well fixed. In other words, the optimal χ parameter fluctuates with cluster size about the optimal value. We have observed similar results on our previous research, for example on aluminum clusters. Many of the medium-sized Al clusters are layered, and so feature GM structures with little strain, which are only predicted at high χ with the Gupta potential; but close to electronic shell closings, where a spherical shape is favoured according to jellium models, a transition towards an spherical and strained GM was observed, implying that the spherical shape favored by an electron shell closing compensates the cost of strain. Now, those structures are only predicted at low χ with the Gupta potential. In words, we believe that electronic shell effects and other effects not included in a Gupta description are the reason that the χ parameter can not have a precisely defined value, and that several potentials about the best average potential should be used to enhance structural diversity.

In our work, we have employed the following: $(\lambda = 0.48, \chi = 2)$, $(\lambda = 0.48, \chi = 10)$, $(\lambda = 0.48, \chi = 50)$, $(\lambda = 0.49, \chi = 2)$. This information does not modify the main message of the paper, but provides the reader with the full details of our procedure.

We expect that it is now fully clear what we mean when stating that $(\lambda = 0.48, \chi = 2)$ is the best potential "on average". It produced the best objective function, which is itself an average of 6 binding energies for different cluster sizes. It is also the potential that proposed structures that converged to the right GM structures in the SIESTA optimizations for most sizes. The choice of $(\lambda = 0.48, \chi = 50)$ may seem strange at first sight as the core repulsion is not so soft anymore. In fact, this potential typically produced structures which were not the GM after SIESTA optimizations, but for example produced the right GM for Zn_{20}. The soft-core potential produces, as explained in the paper, rounded structures while the C_3 GM of Zn_{20} has a rough tetrahedral shape with four "spiky" atoms, and those can only be produced by harder-core potentials. The situation here is similar to the aluminum one mentioned above: the Gupta potential does not incorporate all the essential features of metallic interaction, only some of them, so there seems to be no escape, some flexibility in the χ parameter is advisable. This is an important conclusion that, for brevity reasons, was not exposed enough in the main paper, and is highlighted here.

Acknowledgements: Concerning the TURBOMOLE calculations, the authors acknowledge support by the state of Baden-Wr̈ttemberg through bwHPC.

References

(1) W. Kohn, L. J. Sham, *Phys. Rev.* 1965, **140**, 1133A.

(2) P. Hohenberg, W. Kohn, *Phys. Rev.* 1964, **136**, 864B.

(3) J. M. Soler, E. Artacho, J. D. Gale, A. García, J. Junquera, P. Ordejón, D. Sánchez-Portal, *J. Phys.: Condens. Matter* 2002, **14**, 2475.

(4) J. P. Perdew, A. Zunger, *Phys. Rev. B* 1981, **23**, 5048.

(5) D. M. Ceperley, B. J. Alder, *Phys. Rev. Lett.* 1980, **45**, 566.

(6) J. P. Perdew, K. Burke, M. Ernzerhof, *Phys. Rev. Lett.* 1996, **77**, 3865.

(7) M. Dion, H. Rydberg, E. Schröder, D. C. Langreth, B. I. Lundqvist, *Phys. Rev. Lett.* 2004, **92**, 246401.

(8) G. Román-Pérez, J. M. Soler, *Phys. Rev. Lett.* 2009, **103**, 096102.

(9) J. Klimes, D. R. Bowler, A. Michaelides, *J. Phys.: Condens. Matter* 2010, **22**, 022201.

(10) R. Hamann, M. Schlüter, C. Chiang, *Phys. Rev. Lett.* 1979, **43**, 1494.

(11) L. Kleinman, D. M. Bylander, *Phys. Rev. Lett.* 1982, **48**, 1425.

(12) S. G. Louie, S. Froyen, M. L. Cohen, *Phys. Rev. B* 1982, **26**, 1738.

(13) H. Oymak, S. ErKoc, *Int. J. Mod. Phys. B.* 2012, **26**, 1230003.

(14) C. Kittel, *Introduction to Solid State Physics*, 7th ed. Wiley, New York, 1996.

(15) Janthon, P.; Luo, S.; Kozlov, S. M.; Viñes, F.; Limtrakul, J.; Truhlar, D. G.; Illas, F. *J. Chem. Theory Comput.* **2014**, *10*, 3832-3839.

(16) J. Wang, G. Wang, J. Zhao, *Phys. Rev. A.* 2003, **68**, 013201.

(17) G. Kresse and J. Hafner, *Phys. Rev. B.* 1993, **47**, R558.

(18) G. Kresse and J. Furthmüller, *Phys. Rev. B.* 1996, **54**, 11169.

(19) TURBOMOLE V7.2.1 2017, a development of University of Karlsruhe and Forschungszentrum Karlsruhe GmbH, 1989-2007, TURBOMOLE GmbH, since 2007; available from http://www.turbomole.com.

(20) Gaussian 09, Revision C.01, M. J. Frisch, G. W. Trucks, H. B. Schlegel, G. E. Scuseria, M. A. Robb, J. R. Cheeseman, G. Scalmani, V. Barone, G. A. Petersson, H. Nakatsuji, X. Li, M. Caricato, A. Marenich, J. Bloino, B. G. Janesko, R. Gomperts, B. Mennucci, H. P. Hratchian, J. V. Ortiz, A. F. Izmaylov, J. L. Sonnenberg, D. Williams-Young, F. Ding, F. Lipparini, F. Egidi, J. Goings, B. Peng, A. Petrone, T. Henderson, D. Ranasinghe, V. G. Zakrzewski, J. Gao, N. Rega, G. Zheng, W. Liang, M. Hada, M. Ehara, K. Toyota, R. Fukuda, J. Hasegawa, M. Ishida, T. Nakajima, Y. Honda, O. Kitao, H. Nakai, T. Vreven, K. Throssell, J. A. Montgomery, Jr., J. E. Peralta, F. Ogliaro, M. Bearpark, J. J. Heyd, E. Brothers, K. N. Kudin, V. N. Staroverov, T. Keith, R. Kobayashi, J. Normand, K. Raghavachari, A. Rendell, J. C. Burant, S. S. Iyengar, J. Tomasi, M. Cossi, J. M. Millam, M. Klene, C. Adamo, R. Cammi, J. W. Ochterski, R. L. Martin, K. Morokuma, O. Farkas, J. B. Foresman, and D. J. Fox, Gaussian, Inc., Wallingford CT, 2016.